INL/RPT-24-79415-Revision-0

Effects of N-Doping on Silicon Carbide

July 2024

Changing the World's Energy Future

Kolae Ashlee Knudsen

Idaho National Laboratory

INL/RPT-24-79415-Revision-0

Effects of N-Doping on Silicon Carbide

Kolae Ashlee Knudsen

July 2024

Idaho National Laboratory
Idaho Falls, Idaho 83415

http://www.inl.gov

Prepared for the
U.S. Department of Energy
Under DOE Idaho Operations Office
Contract DE-AC07-05ID14517

Effects of n-Doping on Silicon Carbide

Kolae Knudsen

Abstract

Silicon carbide (SiC) is a widely utilized material within many industries due to its favorable properties, most notably its achieved electrical resistivity at high temperatures, excellent thermal conductivity, and sturdy mechanical properties. The nuclear industry is one of those industries with interest in the applications of SiC. Doping, particularly n-type doping, is shown to significantly reduce electrical resistivity, but due to structural changes within the lattice caused by interaction with neutrons in reactor, it is possible that other attributes of SiC may also be affected. In addition to review of past literature and data, four-point probe testing, scanning electron microscopy, nanoindentation, strength tests, differential scanning calorimetry and laser flash analysis were used to investigate the effects of n-doping in 3C β-phase SiC. According to temperature dependent measurements, electrical resistivity and thermal conductivity both declined as dopant levels increased. Dopant levels are shown to have a significant effect on the mechanical performance of SiC, with the highest dopant levels (4×10^{18} atoms/cm^{-3}) providing a 40% decrease in elastic modulus from 420 GPa to 258 GPa and a 30% decrease in hardness from 40 GPa to 27.7 GPa. These values are still relatively high and doped SiC may prove valuable for nuclear applications.

1. Introduction

For years, the electronics industry has favored silicon carbide (SiC) as the prime semiconductor of choice for many different applications due to its highly advantageous characteristics such as wide band gap energy, modifiable electrical conductivity, and high breakdown voltage [1-6]. Other industries, including automotive, ballistics, and aeronautics, have also been utilizing SiC for its other properties, such as high tensile strength and hardness, extreme resistance to thermal shock, and great thermal conductivity [1-6]. Of particular interest to the nuclear industry are the radiation stability and high thermal conductivity that SiC exhibits. Much research has been dedicated in the nuclear field to investigating intrinsic SiC for applications of accident-tolerant fuel (ATF), reactor control rods, heat control structures, fusion energy blanket and wall structures, and LWR control boxes due to its stability in extreme conditions [1], but there are still investigations to be done.

2. Technical Knowledge

Although pristine SiC has various excellent properties that make it a widely applicable substance for numerous applications, there is a method to precisely adjust its properties. This method is known as doping, a process by which a foreign element is introduced into a chemical structure, replacing some of the atoms in the crystal lattice. By strategically controlling the dopant element, the properties of a material can be enhanced towards specialized scenarios. There are two types of doping: p-type and n-type. P-type doping introduces electron deficient atoms into the crystalline structure which removes electrons from the valence band and creates energy states known as “holes” that diffuse through the material and conduct electricity. N-type doping introduces electron abundant atoms into the crystalline structure that add electrons into the conduction band and these electrons diffuse through the material to conduct electricity. In the case of SiC, boron and aluminum are the most common p-type dopant and nitrogen and phosphorus for n-type doping. In both cases, electrical conductivity is increased.

When doping a material, it may be difficult to ensure an even and homogeneous dispersal of dopant throughout the structure. In a reactor under a neutron flux, silicon-30 can transmute into phosphorus by capturing a neutron which excites the silicon atom, to which it releases a photon and returns to the ground state.

$$^{30}\mathrm{Si} + \mathrm{n} \rightarrow \ ^{31}\mathrm{Si} + \gamma$$

However, silicon-31 is not a stable isotope of silicon, so it decays into a stable isotope of phosphorus, phosphorus-31, emitting a beta particle in the process.

$$^{31}\mathrm{Si} \rightarrow \ ^{31}\mathrm{P} + \beta$$

This procedure is known as neutron transmutation doping (NTD) and it can reduce the irregular distribution of dopant, ensuring homogeneity of the modified properties across the material that may not be reflected in conventional doping methods [2,3]. In addition, because the process is a nuclear transformation on the starting specimen itself and does not involve direct exposure to impurities, it significantly reduces the presence of defects. NTD is a process used for n-type doping, and thus, will be introducing additional electrons into the lattice structure. Silicon has three stable isotopes, silicon-28, silicon-29, and silicon-30, of abundance at 92.8%, 4.7%, and 3.2% respectively, all of which are able to capture neutrons and be transmuted. Within a neutron flux, and particularly with thermal neutrons, SiC undergoes sustained phosphorus doping according to the equation:

$$^{28}\mathrm{Si}\ (n,\gamma)\ ^{29}\mathrm{Si};\ 29\mathrm{Si}(n,\gamma)\ ^{30}\mathrm{Si};$$
$$(n,\gamma) \quad \rightarrow \quad ^{31}\mathrm{P} \ + \ \beta$$

Due to the changes introduced through interaction between lattice atoms and thermal neutrons, other lattice structure dependent properties may be modified as well, such as elastic modulus, tensile strength, and hardness [7,8]. This phenomenon is what we will be investigating and if it proves true, SiC may be the key to optimizing reactor construction and would be of exceptional use to other industries.

3. Methods

There were several properties of interest, most notably electrical resistivity, thermal conductivity, hardness, and elastic modulus. Other properties of note were heat capacity, thermal expansion, Hall coefficient, and yield strength.

All SiC was acquired from the Rohm and Haus chemical vapor deposition (CVD) process, a well-known technique renowned for its ability to produce highly pure material. A purity of > 99.9995% for pure SiC was indicated by the supplier. Although all pre-doped SiC was doped with nitrogen in varying concentrations (see Table 1), all NTD irradiations will result in phosphorus doping. All doping will be n-type. Face centered cubic (FCC) β-phase SiC was chosen for this experiment due to having the smallest band gap energy of the three most common polytypes at 2.36 eV [5]. The grain size for this material is 5 μm.

For several doped samples, annealing was implemented to electrically activate atoms and ensure that given concentrations contributed closer to expected. Previous research indicates that an optimized temperature of approximately 1275°C produced the lowest resistivity in SiC [10]. Consequently, specimens were annealed at 1275°C for 2 hours in an inert, high purity argon atmosphere (99.999%) flowing at 200 SCCM (standard cubic centimeter per minute) to minimize the probability of oxidization. At the time, these samples are still yet to be tested.

Low temperature electrical resistivity and thermal conductivity were measured using the Quantum Design Physical Properties Measurement System (PPMS). A four-contact configuration was utilized to measure electrical properties and a two-contact configuration was used for thermal conductivity. Electrical resistivity measurements were conducted from 3K to 350K at an increasing rate of 0.5K/min. Thermal conductivity measurements were conducted from 2K to 350K also at an increasing rate of 0.5K/min.

In addition, laser flash analysis (LFA) and differential scanning calorimetry (DSC) were used to provide additional information about thermal conductivity. LFA procedures had the system heat to 600°C and then cool down to 0°C two times, stopping at 25°C, 50°C, 100°C, 200°C, 300°C, 400°C, 500°C, and 600°C to take five shots at the specimen. DSC measurements were taken at the same temperature range twice through. Thermal diffusivity and heat capacity were measured with these apparatuses respectively and from there, thermal conductivity was calculated according to the equation:

$$\kappa = \alpha C_p \rho$$

Where α is thermal diffusivity, C_p is specific heat capacity at constant pressure, and ρ is material density (3.21 g/cm^3).

Mechanical properties were measured using several methods, including nanoindentation and standard strength tests using load frames. Nanoindentation loads utilized a Berkovich indenter tip that applied loads of 5000 mN. Load frames were tested at a speed of 0.001mm/min.

Starting undoped specimens were tested alongside irradiated samples to provide benchmark numbers. To prepare the samples for PPMS testing, 3mm discs were cut to 3mm x 1mm x 1mm rectangular prisms via wire cutter. In addition, cylindrical 15mm rods were also tested for thermal conductivity to provide increased accuracy. As for the doped specimens, they were also cut into rectangular prisms (3mm x 1mm x 0.5mm).

Neutron irradiation was conducted in the Advanced Test Reactor (ATR). The irradiation design includes eight capsule assemblies, assigned letters A through H, placed into baskets and loaded into the reactor. All capsules have equivalent numbers of SiC specimens, 24 tensile "dog bone" specimens (16x4x0.5mm), 10 LFA discs (6x1 mm), and 32 SEM/TEM discs (3x0.5 mm). Capsules were loaded with at least one of each nitrogen-doped SiC variety. A nine orders of magnitude range of n-doping resulted. Each capsule was intended be irradiated for a unique period, with capsules A, B, and C having the shortest irradiation time of 63.37 effective full power days (EFPDs) and capsule F having the longest of 720 EFPDs. Capsules are to be removed once they reach target concentration. As such, only capsules A, B, C, and D are available for testing and capsules E, F, G, and H have yet to be removed from reactor and investigated

Table 1. Nitrogen doping concentrations (non-irradiated)

Specimen	1	2	3	4	5	6	7	8
Nitrogen-Doping (atoms/cm^{-3})	4 x 10^9	4 x 10^{10}	4 x 10^{12}	4 x 10^{13}	4 x 10^{14}	4 x 10^{15}	8 x 10^{16}	4 x 10^{18}

Table 2. Targeted phosphorus concentrations and irradiation durations

Capsule	Target P-concentration (atoms/cm^{-3})	EFPDs
Capsule A	2.5E+14	63.37
Capsule B	7.5E+15	63.37
Capsule C	5.3E+16	63.37
Capsule D	3.7E+17	119.3
Capsule E (projection)	1.7E+18	360
Capsule F (projection)	5.9E+18	720
Capsule G(projection)	8.6E+17	240
Capsule H (projection)	6.2E+17	180

4. Results

To effectively analyze the results, undoped SiC specimens were measured to provide benchmark numbers. At room temperature, the electrical resistivity measured to be ~8000 Ω-cm and modeled an exponential downward trend as temperature increased from 250K to 350K. Previous literature has provided 10^2-10^6 Ω-cm and an exponential downward trend as standard [2,4].

Electrical resistivity results mirrored prior research consensus on n-doping in SiC, showing that as doping levels increased, electrical resistivity would decrease. At the highest doping level observed (4×10^{18} atoms/cm^{-3}), resistivity was nearly halved, as ~5000 Ω-cm was measured. Due to the added electrons, it was expected that this value would decrease.

Thermal property results indicated a decrease in heat capacity and thermal diffusivity, resulting in a decrease in thermal conductivity. At 50℃, doped yet unirradiated SiC (4×10^{15} atoms/cm^{-3}) had measured a conductivity of 0.138 W/m-K, while doped and irradiated SiC (3.74×10^{17} atoms/cm^{-3}) had measured a conductivity of 0.00817 W/m-K. It should be noted that the DSC apparatus was unable to measure heat capacity at room temperature (~20℃/300K), which was the metric to be benchmarked. Regardless, across all temperatures, thermal conductivity was noticeably smaller amongst the NTD-doped samples. This consequence is not unforeseen, as marginal decreases in thermal conductivity as a response to irradiation have been previously reported [9, 16]. An increase in porosity as a side effect of irradiation may be cited as the main contributor to this increase, as it is widely accepted that thermal conductivity will degrade with a rise in porosity [9].

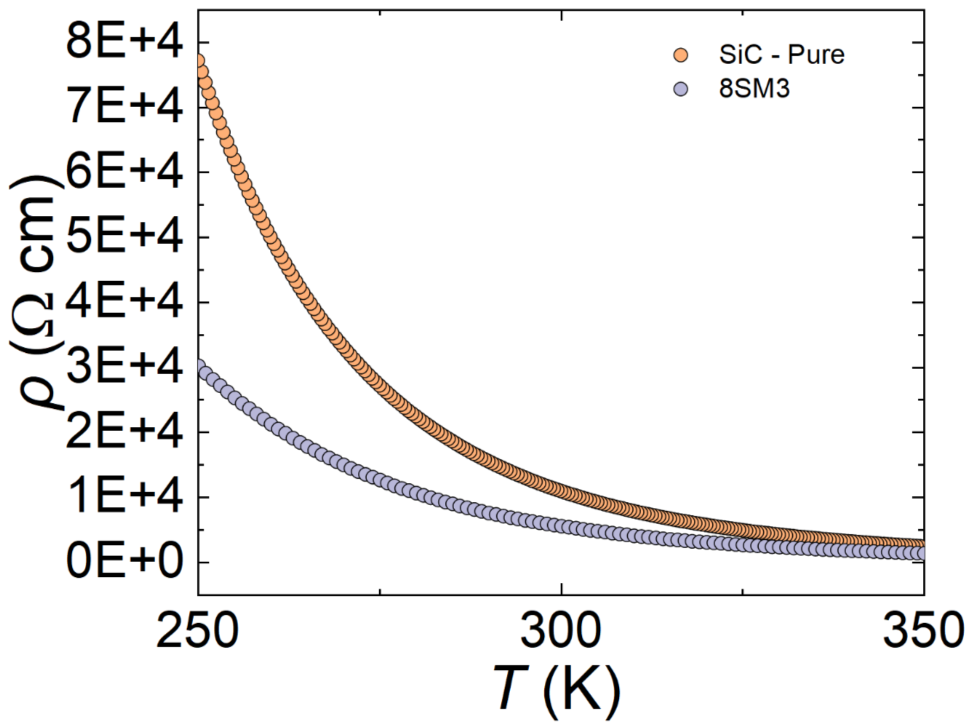

Figure 1. Electrical resistivity results comparison

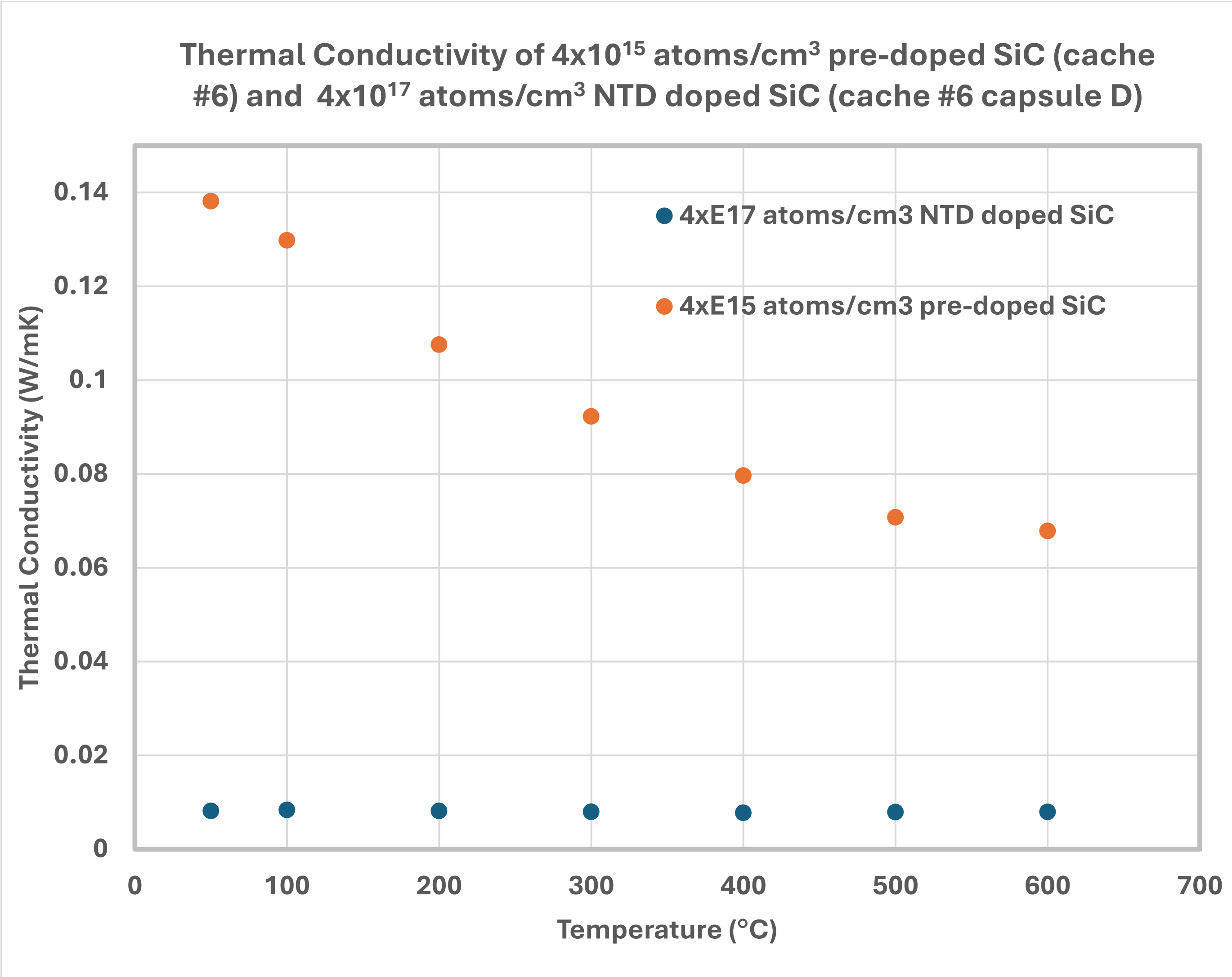

Figure 2. Thermal conductivity results comparison

Nanoindentation results indicated that added dopant provides a slight decrease in elastic modulus and hardness. Typical values of both properties nominally fall around 420 GPa and 40 GPa respectively [11, 12]. Samples with a pre-doped concentration of 4 x 10^{9} atoms/cm^{-3} showed to have an elastic modulus of 328 GPa and a hardness of 30.6 GPa, signifying a 22% reduction in elastic modulus and 23% reduction in hardness. Meanwhile, samples with a pre-doped concentration of 4 x 10^{18} atoms/cm^{-3} had an elastic modulus of 258 GPa and a hardness of 27.7 GPa. Increasing the doping concentration by nine orders of magnitude shows to have reduced the elastic modulus by 20% and the hardness by 10%. Overall, having a moderate dopant dose of 10^{18} atoms/cm^{-3} is shown to have a 40% reduction in elastic modulus and 30% reduction in hardness. Considering that undoped SiC has an exceptionally large elastic modulus and hardness, it is debatable as to whether this is a substantial change, especially compared to other properties such as yield or fracture strength [13]. It is also to note that due to SiC being a highly brittle material, it is possible that there is no correlation between dopant concentration and mechanical performance from these experiments, as mechanical performance can vary wildly [17].

Initially, the scope of strength testing was to measure total yield strength, however, due to the incredibly brittle nature of SiC, only maximum load and ultimate tensile strengths were reported. The mean maximum load across testing was calculated to be 90 N with a standard deviation of 42 N, indicating a wide range of forces across the samples. This is not abnormal for brittle materials [17].

Table 3. Recorded tensile testing results

ID	Width (mm)	Thickness (mm)	Length (mm)	Rate 1 (mm/min)	Maximum Force (N)	UTS (Mpa)	Modulus (Mpa)
1PT1	1.215	0.523	16	0.001	47	73.6	na
2PT1	1.221	0.537	16.008	0.001	65	98.6	na
3PT1							
4PT1	1.215	0.52	16.016	0.001	131	207.6	na
5PT1							
6PT1	1.222	0.515	16.014	0.001	150	237.8	10150
7PT1	1.235	0.546	16.008	0.001	90	133.4	96264
8PT1	1.224	0.522	16.006	0.001	57	88.5	86601
				Mean	90	140	
				StDev	42	68	

It should be noted that several issues were faced during testing. Most importantly, two samples failed prior to collecting any measurements, effectively narrowing the planned sample size by 25%. Sample 3PT1 had arrived broken upon arrival at the facility. Sample 5PT1 had failed during manual adjustments to the system to remove any excess slack. In addition, the pre-loaded process may have exerted additional force before the test began. This is an inherent part of the process to ensure there is no torsional force interfering with results. Therefore, 10 N of pre-loading had to be applied, but that was raised to 25 N to guarantee that the sample would stay stationary. Premature failure and inconsistent results may partially be attributed to this process. However, for current results, the load (N) versus displacement (mm) curve has been adjusted to reflect a zero displacement point at 25 N, thereby removing any unnecessary data before 25 N and normalizing all samples.

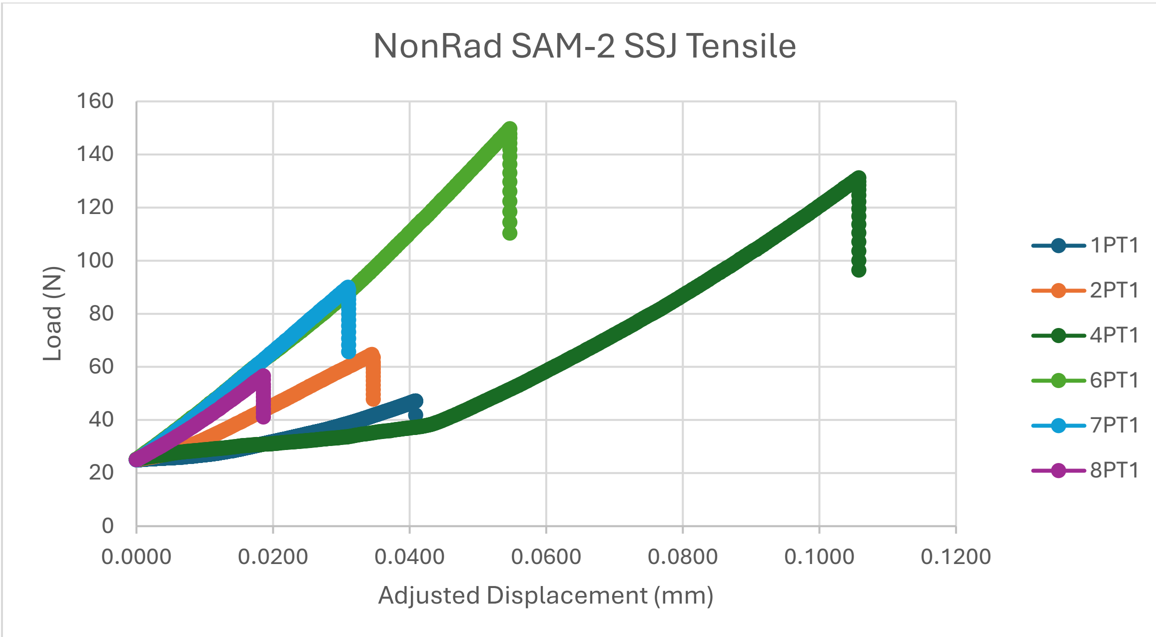

Figure 3. Modified load (N) versus displacement (mm) curve for each sample

5. Conclusions and Discussion

By reviewing the outcomes of n-doping in 3C-SiC, decreased values in several thermal and mechanical properties and improved values for electronic properties were found when SiC was doped. The elastic modulus and hardness of the material showed a 40% and 30% reduction respectively when 4 x 10^{18} atoms/$cm^{-3}$of nitrogen doping was measured, illustrating that at moderate doping concentrations, degradation of mechanical performance has occurred, though the effects may be relatively negligible when used for certain applications. Moving forward, the methods by which mechanical testing is performed will be investigated thoroughly and improved to better accommodate the material. Standard strength testing does not provide enough consistency to confidently relay any findings. The loading process is just simply too involved. To get an accurate strength test, the sample must be perfectly aligned in all axes, as any non-axial force applied may create torque, causing additional strain on the specimen. So, to ensure no extraneous loads prior to sample recollection is involved, alignment must be applied in the form of loading jaws [14]. Putting these on can cause small and fragile samples to break, as seen with the sample 5PT1. As such, other practices must be employed.

The first solution is to implement three- or four-point bend testing, preferably four-point. Four-point bend tests offer a more accurate measurement of ultimate tensile strength in ceramics, since force is dispersed over a longer length as opposed to the centralized stress location of three- point test or standard tensile test, majorly avoiding the fear of premature failure [15]. Bend tests also have a simpler loading procedure. There is no manual supervision over torque, as the bend points are already parallel, ensuring fully uniaxial force and that no torsion force will be applied to the fragile samples.

Another solution is micro-cantilever testing. Like the bend testing, there is little risk of failure from loading. In addition, another characteristic would be acquired: fracture strength. Since the procedure creates a crack initiating point at the base of the specimen, the behavior of the material with preexisting deformities would be observed.

From the current results, doped SiC has a decrease in thermal conductivity and mechanical properties, but is still incredibly strong and its values are even with or far exceed many materials. This material could be promising for high-temperature nuclear applications.

Acknowledgements

Thank you to the following researchers and contributors: Volodymyr Buturlim, Sabin Regmi, Scott Middlemas, Craig Marshall, and George Evans. A very special thank you to my mentor Rory Kennedy for providing me this opportunity to learn and work alongside him and everyone else I met during my time here at the INL.

References

[1] Y. Katoh, L. Snead, Silicon carbide and its composites for nuclear applications – Historical overview, Journal of Nuclear Materials, Vol. 526 (2019).

[2] A. Carbonari, Neutron transmutation doping of silicon: highly homogeneous resistivity semiconductor material produced in nuclear reactors, Proceedings of the 4 Brazilian meeting on nuclear applications, Vol. 2 (1997).

[3] B. Park, G. Kang, J. Park, Test of neutron transmutation doping of SiC by implantation of phosphorus, Transactions of the Korean Nuclear Society Spring Meeting (2022).

[4] L. Snead, T. Nozawa, Y. Katoh, T. Byun, S. Kondo, D. Petti, Handbook of SiC properties for fuel performance modeling, Vol. 371. (2007).

[5] M. Levinshtein, S. Rumyanstev, M. Shur, Properties of Advanced Semiconductor Materials (2001).

[6] H. Xiong, W. Mao, R. Wang, S. Liu, N. Zhang, L. Song, D. Yang, X. Pi, Characterizations on the doping of single-crystal silicon carbide, Materials Today Physics, Vol. 29 (2022).

[7] N. Top, I. Şahin, H. Gökçe, The Mechanical Properties of Functionally Graded Lattice Structures Derived Using Computer-Aided Design for Additive Manufacturing. Appl. Sci., Advanced Manufacturing Technologies and Their Applications, Vol. 2 (2023).

[8] T. Maconachie, M. Leary, B. Lozanovski, X. Zhang, M. Qian, O. Faruque, M. Brandt, SLM lattice structures: Properties, performance, applications and challenges, Materials & Design, Vol. 183 (2013).

[9] S. Kultayeva, Y. Kim, I. Song, Effects of dopants on electrical, thermal, and mechanical properties of porous SiC ceramics, Journal of the European Ceramic Society Vol. 41 (2021).

[10] F. Li, Y. Sharma, V. Shah, M. Jennings, A. Pérez-Tomás, M. Myronov, C. Fisher, D. Leadley, P. Mawby, Electrical activation of nitrogen heavily implanted 3C-SiC(100), Applied Surface Science, Vol. 353 (2015).

[11] L. Zhao, J. Zhang, J. Pfetzing, M. Alam, A. Hartmaier, Depth-sensing ductile and brittle deformation in 3C-SiC under Berkovich nanoindentation, Materials & Design, Vol. 197 (2021).

[12] L. Vargas-Gonzales, R. Speyer, J. Campbell, Flexural Strength, Fracture Toughness, and Hardness of Silicon Carbide and Boron Carbide Armor Ceramics, Vol. 7 (2010).

[13] W. Dienst, Mechanical properties of neutron-irradiated ceramic materials, Journal of Nuclear Materials, Vol. 211 (1994).

[14] A. Heyer, A. Bracq, J. Rossit, F. Moitrier, G. Gütter, F. Delorme, S. Lemonnier, Methodology for strength distribution estimation of ceramics from ball-on-three-balls and four-point bending experiments, Weibull statistics and fractographic investigations: Application to magnesium aluminum spinel, Ceramics International, Vol. 49 (2023).

[15] X. Han, Q. Xiao, K. Cui, X. Hu, Z. Zhou, Determining the fracture toughness of quasi-brittle materials with notched four-point bending tests, Engineering Fracture Mechanics, Vol. 284 (2023).

[16] Y. Katoh, T. Nozawa, C. Shih, K. Ozawa, T. Koyanagi, W. Porter, L. L. Snead,

High-dose neutron irradiation of Hi-Nicalon Type S silicon carbide composites. Part 2: Mechanical and physical properties, Journal of Nuclear Materials, Vol. 462 (2015).

[17] D. Leguillon, É. Martin, M.C. Lafarie-Frenot, Flexural vs. tensile strength in brittle materials, Comptes Rendus Mécanique, Vol. 343 (2015)